UDK 620.1/.2:620.19:532.6
Original scientific article/Izvirni znanstveni članek

ISSN 1580-2949
MTAEC9, 51(6)1043(2017)

COMPARISON OF THE SURFACE AND ANTICORROSION PROPERTIES OF SiO_2 AND TiO_2 NANOPARTICLE EPOXY COATINGS

PRIMERJAVA POVRŠINSKIH IN PROTIKOROZIJSKIH LASTNOSTI EPOKSIDNIH PREVLEK OBOGATENIH S SiO_2 IN TiO_2 NANOVKLJUČKI

Marjetka Conradi, Aleksandra Kocijan

Institute of Metals and Technology, Lepi pot 11, 1000 Ljubljana, Slovenia
marjetka.conradi@imt.si

Prejem rokopisa – received: 2017-08-21; sprejem za objavo – accepted for publication: 2017-10-02

doi:10.17222/mit.2017.137

In this article we compare the morphology, wetting and anticorrosion properties of fluorosilane-modified TiO_2, FAS-TiO_2/epoxy and SiO_2, FAS-SiO_2/epoxy coatings. Thirty-nanometre TiO_2 and SiO_2 nanoparticles were spin coated onto the AISI 316L steel substrate and covered with a thin epoxy layer for nanoparticle fixation. The morphology of the coatings was analysed with SEM imaging and the average surface roughness (S_a), and it showed a homogeneous FAS-TiO_2 nanoparticle distribution in the coating, whereas the FAS-SiO_2 nanoparticles tended to agglomerate. Static water contact angles were measured to evaluate the wetting properties, indicating the highly hydrophobic nature of both coatings. Potentiodynamic measurements showed that the addition of nanoparticles to the epoxy coating significantly improved the corrosion resistance of the AISI 316L stainless steel.

Keywords: TiO_2, SiO_2, epoxy, coatings, wetting, corrosion

V članku primerjamo morfologijo, omočitvene lastnosti in antikorozijske lastnosti s fluorosilanom oblečenih TiO_2, FAS-TiO_2/epoksi in SiO_2, FAS-SiO_2/epoxy prevlek. 30-nm TiO_2 in SiO_2 nanodelce smo na jekleno podlago tipa AISI 316L nanesli s "spin coaterjem" ter jih prekrili s tanko plastjo epoksidne smole, ki je zagotovila fiksacijo nanodelcev na površini. Morfološke lastnosti prevlek smo analizirali s SEM mikroskopijo ter z meritvami povprečne hrapavosti površine (S_a). Pokazali smo, da so FAS-TiO_2 nanodelci v prevleki enakomerno razporejeni, medtem, ko FAS-SiO_2 nanodelci kažejo visoko stopnjo aglomeracije. Omočitvene lastnosti prevlek smo določili z meritvami statičnih kontaktnih kotov, ki so pokazale hidrofobne lastnosti tako FAS-TiO_2/epoksi kot tudi FAS-SiO_2/epoksi prevlek. Potenciodinamske meritve potrjujejo, da z dodatkom nanodelcev epoksi, zaščitnim prevlekam izrazito izboljšamo korozijsko obstojnost nerjavnega jekla AISI 316L.

Ključne besede: TiO_2, SiO_2, epoksi, prevleke, omočitvene lastnosti, korozija

1 INTRODUCTION

Designing a solid surface with specific surface characteristics, such as wetting properties, mechanical resistance, anticorrosion properties, etc., is challenging in several applications in aerospace, marine, biomedicine etc[1,2]. Therefore, the surface modification of engineering metallic materials, such as the most commonly used austenitic stainless steel (AISI),[3,4] by various coatings represents an important subject in the field of enhancing particular surface properties, mechanical as well as anticorrosion properties.

Epoxy coatings serve as an excellent physical barrier for metallic surface protection due to their good mechanical and electrical insulating properties, chemical resistance and strong adhesion to different substrates. However, the highly cross-linked structure of an epoxy resin often makes epoxy coatings susceptible to the propagation of cracks and damage by surface abrasion and wear.[5] It has been shown that the implementation of various nanoparticles like SiO_2, TiO_2, ZnO, CuO, etc. additionally improves the performance of coatings.[6] Nanoparticles also enhance the corrosion protection properties of the epoxy coatings by decreasing the porosities due to the small size and high specific area.

The hierarchical structures of nanoparticle/epoxy composites can, on the other hand, also change the wetting characteristics of the surface. It is well known that the surface roughness can enhance both hydrophobicity and hydrophilicity.[7,8] In combination with the nanoparticle surface chemistry (i.e., functionalization) we can control the wetting characteristics of epoxy coatings[9] that additionally allows for an improvement of the anticorrosion properties.

Here we report on a comparison of the surface and anticorrosion properties of hydrophobic FAS-TiO_2/epoxy and FAS-SiO_2/epoxy coatings. The morphology and wetting properties are characterized as well as the anticorrosion properties through potentiodynamic measurements.

2 EXPERIMENTAL PART

Materials. Austenitic stainless steel AISI 316L (17 % Cr, 10 % Ni, 2.1 % Mo, 1.4 % Mn, 0.38 % Si, 0.041 % P,

0.021 % C, <0.005 % S in mass fraction) was used as a substrate.

A biocompatible epoxy EPO-TEK 302-3M (EPOXY TECHNOLOGY, Inc.) was mixed in the producer-prescribed two-component *w*/% ratio 100:45. 30-nm TiO_2 nanoparticles with mean were provided by Cinkarna Celje, whereas the 30-nm SiO_2 nanoparticles were supplied by Cab-O-Sil.

Surface functionalization. For hydrophobic effect as well as for homogenization of nanoparticle distribution, SiO_2 and TiO_2 particles were functionalized in 1 % of volume fractions of ethanolic fluoroalkylsilane or FAS17 ($C_{16}H_{19}F_{17}O_3Si$) solution.

Steel substrate preparation. Prior to the application of the coating, the steel discs of 25 mm diameter and with a thickness of 1.5 mm were diamond polished following a standard mechanical procedure and then cleaned with ethanol in an ultrasonic bath.

Coating preparation. To improve the SiO_2 and TiO_2 nanoparticles' adhesion, the diamond-polished AISI 316L substrate was spin-coated with a thin layer of epoxy and then cured for 3 h at 65 °C. To ensure good surface coverage, five drops (20 µL) of 3 % of mass fractions of TiO_2/SiO_2 nanoparticle ethanolic solution were then spin-coated onto an epoxy-coated AISI 316L substrate and dried in an oven for approximately 20 min at 100 °C. Finally, the coatings were covered with another thin layer of epoxy for particle fixation and then cured for 3 h at 65 °C.

Scanning electron microscopy (SEM). SEM analysis using FE-SEM Zeiss SUPRA 35VP was employed to investigate the morphology of the nanoparticle coatings' surfaces, which were sputtered with gold prior to imaging.

Contact-angle measurements. The static contact-angle measurements of water (W) on the nanoparticle coatings were performed using a surface-energy evaluation system (Advex Instruments s.r.o.). Liquid drops of 5 µL were deposited on different spots of the substrates to avoid the influence of roughness and gravity on the shape of the drop. The drop contour was analysed from the image of the deposited liquid drop on the surface and the contact angle was determined by using Young-Laplace fitting. To minimize the errors due to roughness and heterogeneity, the average values of the contact angles of the drop were calculated approximately 30 s after the deposition from at least five measurements on the studied coated steel. All the contact-angle measurements were carried out at 20 °C and ambient humidity.

Surface roughness. Optical 3D metrology system, model Alicona Infinite Focus (Alicona Imaging GmbH), was used for the surface-roughness analysis. At least three measurements per sample were performed at a magnification of 20× with a lateral resolution of 0.9 µm and a vertical resolution of about 50 nm. IF-Measure-Suite (Version 5.1) software was later on used to calculate the average surface roughness, S_a, for each sample, based on the general surface-roughness equation (Equation (1)):

$$Sa = \frac{1}{L_x}\frac{1}{L_y}\int_0^{L_x}\int_0^{L_z}\left|z(x,y)\right|\mathrm{d}x\mathrm{d}y \qquad (1)$$

where L_x and L_y are the acquisition lengths of the surface in the x and y directions and $z(x,y)$ is the height. The size of the analysed area was 1337×540 µm^2.

Electrochemical measurements. Electrochemical measurements were performed on the epoxy-coated, FAS-SiO_2/epoxy-coated and FAS-TiO_2/epoxy-coated AISI 316L stainless steel in a simulated physiological Hank's solution, containing 8 g/L NaCl, 0.40 g/L KCl, 0.35 g/L $NaHCO_3$, 0.25 g/L $NaH_2PO_4{\cdot}2H_2O$, 0.06 g/L $Na_2HPO_4{\cdot}2H_2O$, 0.19 g/L $CaCl_2{\cdot}2H_2O$, 0.41 g/L $MgCl_2{\cdot}6H_2O$, 0.06 g/L $MgSO_4{\cdot}7H_2O$ and 1 g/L glucose, at pH = 7.8 and 37 °C. All the chemicals were from Merck, Darmstadt, Germany. The measurements were performed by using BioLogic Modular Research Grade Potentiostat/Galvanostat/FRA Model SP-300 with an EC-Lab Software and a three-electrode flat corrosion cell, where the working electrode (WE) was the investigated specimen, the reference electrode (RE) was a saturated calomel electrode (SCE, 0.242 V vs. SHE) and the counter electrode (CE) was a platinum net. The potentiodynamic curves were recorded at the open-circuit potential (OCP), starting the measurement at 250 mV vs. SCE more negative than the OCP. The potential was increased using a scan rate of 1 mV s^{-1}.

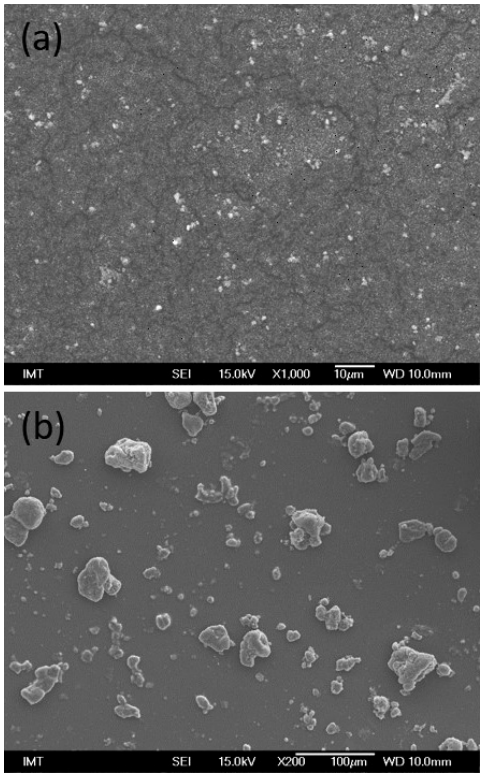

Figure 1: SEM images of the surface morphology of: a) FAS-TiO_2/epoxy and b) FAS-SiO_2/epoxy coatings

3 RESULTS AND DISCUSSION

3.1 Surface morphology

Figure 1 compares the morphology of the FAS-TiO_2/epoxy and FAS-SiO_2/epoxy coatings. The SEM images reveal a distinctive morphology between the two coatings that is reflected in the different length scale of the agglomerate formation, which is also reflected in a discrepancy in the average surface roughness S_a (**Table 1**). FAS-TiO_2/epoxy coatings (**Figure 1a**) are characterized with a more refined structure that is a consequence of the better FAS-TiO_2 nanoparticle dispersion with less agglomeration on the micrometre scale. FAS-SiO_2/epoxy coatings, in contrast, are characterized by severe agglomeration (**Figure 1b**) and randomly distributed agglomerates from nanometres to a few micrometres in diameter. This suggests that the FAS functionalization works well with homogenization of TiO_2 nanoparticle distribution, but has no effect on the homogenization of the SiO_2 nanoparticle distribution.

3.2 Wetting properties

To analyse the surface wettability, we performed five static contact-angle measurements with water (W) on different spots all over the sample and used them to determine the average contact-angle values of the coating with an estimated error in the reading of $\theta \pm 1.0°$.

In the first step we prepared the superhydrophobic FAS-TiO_2 and FAS-SiO_2 surfaces by spin-coating the AISI+epoxy substrate with FAS-TiO_2 and FAS-SiO_2 nanoparticles. The corresponding static water contact angles are reported in **Table 1**. Nanoparticle fixation with a thin layer of hydrophilic epoxy ($\theta^w = 71.8°$) eliminated the superhydrophobic effect; however, a substantial degree of hydrophobicity that is necessary for desirable anticorrosion properties[10] was retained, as reported in **Table 1**. The retained high degree of hydrophobicity is most probably a combination of surface roughness and the originally superhydrophobic nature of the FAS-TiO_2 and FAS-SiO_2 nanoparticles. In addition, the top layer of epoxy also smoothened the coating, which is reflected in the reduced average surface roughness, S_a, of the AISI+epoxy+TiO_2/SiO_2+epoxy surfaces compared to the AISI+epoxy+TiO_2/SiO_2 surfaces. This is most probably due to the fact that epoxy fills the space between the nanoparticle agglomerates and reduces the height variation over the whole surface, and therefore also S_a.

There is, however, a noticeable difference in the static water contact angles and a difference by a factor of 10 in the value of the average surface roughness, S_a, As reported in **Table 1**, the FAS-SiO_2/epoxy coating is rougher and more hydrophobic compared to the FAS-TiO_2/epoxy coating. The difference in the average surface roughness was already expected from the surface morphology analysis (**Figure 1**) due to the severe SiO_2 nanoparticle agglomeration compared to the TiO_2 coated surface. The increased hydrophobicity of the FAS-SiO_2/epoxy coating can, on the other hand, be attributed to the more pronounced micro- to nanoparticle-textured surface with a refined roughness structure.[9]

Table 1: Comparison of the static water contact angles (θ^W) and the average surface roughness (S_a) of the FAS-TiO_2/epoxy and FAS-SiO_2/epoxy coatings

Substrate	Contact angle θ^w (°)	Roughness S_a (µm)
epoxy	71.8	0.02
AISI+epoxy+TiO_2	150.1	0.41
AISI+epoxy+SiO_2	155.4	3.69
AISI+epoxy+TiO_2+epoxy	121.1	0.23
AISI+epoxy+SiO_2+epoxy	130.6	2.34

3.3 Potentiodynamic measurements

Figure 2 shows the potentiodynamic behaviour of the FAS-TiO_2/epoxy-coated, FAS-SiO_2/epoxy-coated and epoxy-coated AISI 316L stainless steel in a simulated physiological Hank's solution. The polarization and the passivation behaviour of the tested material after the surface modification was studied. The corrosion potential (E_{corr}) for the epoxy coating in the Hank's solution was approximately –256 mV vs. SCE, for the FAS-TiO_2/epoxy-coated AISI 316L it was –335 mV vs. SCE and for FAS-SiO_2/epoxy-coated AISI 316L it was –407 mV vs. SCE. After the Tafel region, the investigated sample exhibited a broad passive range followed by the breakdown potential (E_b). The passivation range of the FAS-TiO_2/epoxy-coated and FAS-SiO_2/epoxy-coated AISI 316L specimen was moved to the significantly lower corrosion-current densities compared to the pure epoxy-coated AISI 316L. We established that the addition of nanoparticles to the epoxy coating significantly

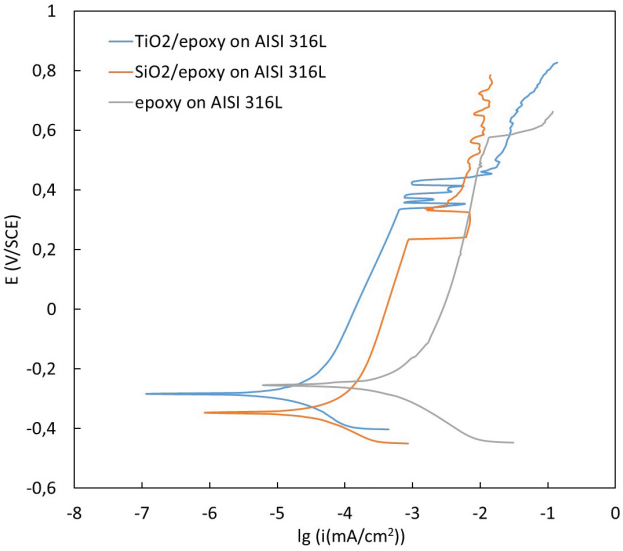

Figure 2: Potentiodynamic curves for FAS-TiO_2/epoxy-coated, FAS-SiO_2/epoxy-coated and epoxy-coated AISI 316L substrate in a simulated physiological Hank's solution

enhanced the corrosion resistance of the AISI 316L stainless steel compared to the pure epoxy coating, especially in the case of the FAS-TiO_2/epoxy coating. The corrosion parameters calculated from the potentiodynamic measurements showed decreased corrosion-current densities and increased the polarisation resistances of the specimens coated with FAS-TiO_2/epoxy and FAS-SiO_2/epoxy coating compared to the pure epoxy coating (**Table 2**). The superior protective properties of the FAS-TiO_2/epoxy coating were attributed to the more uniform distribution of the FAS-TiO_2 nanoparticles within the coating.

Table 2: Corrosion parameters calculated from the potentiodynamic measurements

Material	$E(I=0)$ (mV)	I_{corr} (μA)	R_p (kΩ)	v_{corr} (nm/year)
epoxy coated AISI 316L	–256	0.33	78	1.1
SiO_2/epoxy coated AISI 316L	–407	0.06	557	0.7
TiO_2/epoxy coated AISI 316L	–335	0.02	1500	0.2

4 CONCLUSIONS

We analysed the morphology of FAS-TiO_2/epoxy and FAS-SiO_2/epoxy coatings showing that the FAS functionalization works well with the homogenization of the TiO_2 nanoparticle distribution, but has no effect on the homogenization of the SiO_2 nanoparticle distribution, as these tend to agglomerate. This is directly reflected in the SEM image analysis and the average surface-roughness measurements. The wetting properties evaluation reveals the superhydrophobic nature of the FAS-TiO_2 and FAS-SiO_2 nanoparticle coatings prior to the epoxy layer's deposition for the nanoparticle fixation. This suggests that hydrophilic epoxy eliminates the superhydrophobic effect, retaining, however, a high degree of hydrophobicity that is a consequence of the combination of surface roughness and the originally superhydrophobic nature of the FAS-TiO_2 and FAS-SiO_2 nanoparticles. There is also a noticeable difference in the static water contact angles between the FAS-TiO_2/epoxy and the FAS-SiO_2/epoxy coatings, the FAS-SiO_2/epoxy coatings being more hydrophobic due to the more pronounced micro- to nanoparticle-textured surface with a refined roughness structure. The corrosion evaluation showed the significantly enhanced corrosion resistance of the AISI 316L stainless steel with the addition of nanoparticles to the epoxy coating compared to the pure epoxy coating, especially in the case of the FAS-TiO_2/epoxy coating. The uniform distribution of the FAS-TiO_2 nanoparticles within the coating plays a crucial role in the superior protective properties of the coating.

Acknowledgements

This work was carried out within the framework of the Slovenian research project J2-7196: Antibakterijske nanostrukturirane zaščitne plasti za biološke aplikacije, financed by the Slovenian Research Agency (ARRS).

5 REFERENCES

[1] B. Xue, L. Gao, Y. Hou, Z. Liu, L. Jiang, Temperature Controlled Water/Oil Wettability of a Surface Fabricated by a Block Copolymer: Application as a Dual Water/Oil On–Off Switch, Adv. Mater., 25 (**2013**), 278–283, doi:10.1002/adma.201202799

[2] Y. Tian, B. Su, L. Jiang, Interfaces: Interfacial Material System Exhibiting Superwettability, Adv. Mater., 26 (**2014**), 6872, doi:10.1002/adma.201470276

[3] M. A. M. Ibrahim, S. S. A. El Rehim, M. M. Hamza, Corrosion behavior of some austenitic stainless steels in chloride environments, Mat. Chem. Phys., 115 (**2009**), 80–85, doi:10.1016/j.matchemphys.2008.11.016

[4] T. Hryniewicz, R. Rokicki, K. Rokosz, Corrosion characteristics of medical-grade AISI Type 316L stainless steel surface after electropolishing in a magnetic field, Corrosion 64, (**2008**), 660–665, doi:10.5006/1.3279927

[5] B. Wetzel, F. Haupert, M. Q. Zhang, Epoxy nanocomposites with high mechanical and tribological performance, Comp. Sci. Technol. 63, (**2003**), 2055–2067, doi:10.1016/s0266-3538(03)00115-5

[6] Y. Qing, Facile fabrication of superhydrophobic surfaces with corrosion resistance by nanocomposite coating of TiO_2 and polydimethylsiloxane. Colloids and Surfaces a-Physicochemical and Engineering Aspects, 484 (**2015**), 471–477, doi:10.1016/j.colsurfa.2015.08.024

[7] R. N. Wenzel, Resistance of solid surfaces to wetting by water, Ind. Eng. Chem., 28 (**1936**), 988–944, doi: 10.1021/ie50320a024

[8] C. S. Baxter, Wettability of porous surfaces, Trans. Faraday Soc., 40 (**1944**), 546–551

[9] M. Conradi, A. Kocijan, Fine-tuning of surface properties of dual-size TiO_2 nanoparticle coatings. Surface & coatings technology, 304 (**2016**), 486–491, doi:10.1016/j.surfcoat.2016.07.059

[10] Y. Qian, Y. Li, S. Jungwirth, N. Seely, Y. Fang, X. Shi, The Application of Anti- Corrosion Coating for Preserving the Value of Equipment Asset in Chloride-Laden Environments: A Review, Int. J. Electrochem. Sci., 10 (**2015**), 10756–10780